RM-A57I09

RM A57I09

NACA RM A57I09

NACA

RESEARCH MEMORANDUM

EFFECTS OF STING-SUPPORT INTERFERENCE ON THE DRAG OF AN OGIVE-CYLINDER BODY WITH AND WITHOUT A BOATTAIL AT 0.6 TO 1.4 MACH NUMBER

By George Lee and James L. Summers

Ames Aeronautical Laboratory
Moffett Field, Calif.

NATIONAL ADVISORY COMMITTEE FOR AERONAUTICS

WASHINGTON

December 3, 1957

NATIONAL ADVISORY COMMITTEE FOR AERONAUTICS

RESEARCH MEMORANDUM

EFFECTS OF STING-SUPPORT INTERFERENCE ON THE DRAG OF AN OGIVE-CYLINDER BODY WITH AND WITHOUT A BOATTAIL AT 0.6 TO 1.4 MACH NUMBER

By George Lee and James L. Summers

SUMMARY

Tests were conducted to determine the effects of sting-support interference on the zero-lift drag of two bodies of revolution (with and without boattailing). The sting support consisted of a constant-diameter sting followed by a sting flare terminating in a cylindrical support. Various sting diameters, sting lengths, and sting flare angles were tested at Mach numbers of 0.6 to 1.4 and a Reynolds number of 8 million, based on model length.

In general, the addition of the sting support caused a foredrag reduction and a decrease in base drag. The maximum interference occurred at high subsonic speeds. At supersonic speeds, the interference decreased rapidly and approached zero at a Mach number of 1.4.

For the model with boattailing supported on a 1-inch-diameter sting with a 12° flare angle, both foredrag and base drag were affected by changes in sting length when the sting length was less than 6.0 and 6.5 base diameters, respectively. The foredrag and base drag were affected by changes in sting diameter for the entire range of Mach numbers.

For the model with the cylindrical afterbody, the foredrag was not affected by the sting support. However, the base drag was dependent on the sting diameter, but was independent of changes in sting length for lengths greater than 5.5 base diameters.

INTRODUCTION

The importance of understanding the effects of model support interference on wind-tunnel test results has long been recognized. This problem has been extensively studied at subsonic and supersonic speeds.

However, with the recent development of the transonic wind tunnel, the problem of support interference must be considered at transonic speeds. Information presented in references 1 to 6 shows that sting-support interference is considerable, but adequate information for the design of interference-free sting-support systems is lacking. The purpose of the investigation reported herein was to obtain adequate information for the design of minimum interference sting-support systems for a boattail and a cylindrical body with turbulent boundary layer at Mach numbers from 0.6 to 1.4.

SYMBOLS

A frontal area of model

A_B base area of model

C_{D_F} foredrag coefficient, $\frac{\text{total drag minus base drag}}{q_\infty A}$

C_{D_B} base drag coefficient, $-\frac{p_B - p_\infty}{q_\infty}\frac{A_B}{A}$

$C_{D_{BT}}$ boattail drag coefficient, $2\pi\int_{r=1.000}^{r=0.575} C_p r\,dr$, pressure drag over boattail section (does not include base drag)

C_p pressure coefficient, $\frac{p - p_\infty}{q_\infty}$

d diameter of the sting

D maximum diameter of the model (See fig. 1.)

l sting length of constant diameter between model base and sting flare

L model length

M Mach number

p static pressure

q dynamic pressure

r radius of body

x distance from model nose

θ semivertex angle of the sting flare

Subscripts

B base

∞ free stream

cr critical

APPARATUS AND MODELS

The investigation was conducted in the Ames 2- by 2-foot transonic wind tunnel which is described in reference 7. The wind tunnel is of the closed-circuit, variable-density type which employs a perforated test section for continuous transonic speed operation.

Geometric details of the two models used in the investigation are presented in figure 1. Both models had a fineness ratio of 10 with Kármán ogive noses 50 percent of the body length. The boattail model (boattail from 80 to 100 percent of the body length) had a base-diameter to maximum-diameter ratio of 0.575. The slope of the boattail at the base is zero. For pressure measurements, 56 orifices of 0.02-inch diameter were installed longitudinally along both models as shown in figure 1.

For the investigation, the models were supported by various sting-support configurations and by a side support. A photograph of these supports is shown in figure 2. A sketch of a typical sting-support configuration is shown in figure 3. The sting support consisted of a constant-diameter sting followed by a sting flare terminating in a 2-1/2-inch cylindrical support. For the side support plus sting configurations only the 12° sting flare was used.

Total drag measurements were made by means of an internal strain-gage balance. Base pressure (i.e., base drag) was obtained by an orifice inside the base of the models. Model pressures were indicated by a liquid-in-glass manometer and recorded photographically.

TESTS AND DATA REDUCTION

The models were tested at zero angle of attack throughout the Mach number range of 0.60 to 1.4, inclusive. The Reynolds number was 8 million, based on model length. Total drag and base pressure were measured when the models were sting supported. When the side support was employed (with or without stings), base-pressure and afterbody-pressure distributions were measured. The boundary-layer transition point was fixed at 20 percent of the body length on both models by a ring made of 0.032 inch by 0.032 inch brass. The various sting configurations which were tested are listed in figure 3.

Subsonic wall-interference effects, as shown in reference 7, were small enough to require no corrections. Interference caused by wall-reflected shock waves at Mach numbers of 1.06 to 1.15 are known to be present; however, no assessment of their effects has been made.

Apart from possible systematic errors resulting from neglecting the above corrections, the probable errors in the data, as determined by a root-mean-square analysis of data scatter, are considered to be as follows:

$$C_{D_F} = \pm 0.005$$

$$C_{D_B} = \pm 0.004$$

$$M = \pm 0.003$$

RESULTS AND DISCUSSION

The interference created by a sting support has been shown in reference 1 to result from two causes. These are, first, the interference to the flow resulting from the proximity of the sting flare, referred to as the "length effect," and, second, the interference to the flow resulting from the presence of the constant diameter sting, referred to as the "diameter effect." It is known that these two interference effects have critical limits. These are, first, the critical sting-length to base-diameter ratio $(l/D_B)_{cr}$, defined as the minimum l/D_B for obtaining the same C_{D_F} or C_{D_B} as would be obtained for an "infinite" length sting, and, second, the critical sting-diameter to base-diameter ratio $(d/D_B)_{cr}$, defined as the maximum d/D_B for obtaining the same C_{D_F} or C_{D_B} as would be obtained for a sting of zero diameter.

Effect of Sting Length

Boattail model.- The variations of drag coefficient with l/D_B for the 1/2- and 1-inch-diameter stings are presented in figures 4(a) and (b), respectively. It is seen that the sting interference caused a reduction of foredrag coefficient. The magnitude of this interference increased from 0.6 Mach number and reached a maximum near sonic speed. With furthur increase in speed, the interference diminished quite rapidly. As would be expected, the magnitude of the interference due to length effect was amplified by the increased sting flare angle.

The variations of $(l/D_B)_{cr}$ for foredrag with Mach number for the 1/2- and 1-inch-diameter stings are presented in figures 5(a) and (b), respectively. Critical values of l/D_B increased slightly with increasing speeds to a maximum at approximately 0.95 Mach number. With further increase in speed, $(l/D_B)_{cr}$ decreased very rapidly. It is also noted that the values of $(l/D_B)_{cr}$ of the 1-inch-diameter sting were greater than those of the 1/2-inch-diameter sting. The critical values of l/D_B of this investigation for a body of revolution are in good agreement with those of reference 1 for a wing-body model.

Typical pressure distribution measurements for three values of l/D_B are presented in figure 6. The interference, in the form of pressure disturbances, was propagated upstream for a considerable distance at subsonic speeds, but was limited to the rear of the model at supersonic speeds. The magnitudes of these disturbances were progressively diminished with upstream distance.

Typical variations of the base drag coefficient with l/D_B are shown in figure 7. A decrease in sting length caused a decrease in base drag coefficient, the magnitude of which increased with sting flare angle. Theoretically, the sting flare can be represented by a distribution of sources whose strengths are determined by the sting flare size. Tunnell, in reference 1, showed that by this method the $(l/D_B)_{cr}$ for base drag could be estimated at subsonic speeds. This theoretical estimate is shown in figure 7 for $\theta = 12^\circ$. It is seen that the theoretical $(l/D_B)_{cr}$ compare quite well with the experimental values. As mentioned in reference 7, numerical agreement of base drag would not be expected since the theory neglected the presence of the model.

The variations of $(l/D_B)_{cr}$ for base drag coefficient with Mach number are presented in figure 8. It is seen that the values of $(l/D_B)_{cr}$ for base drag are approximately 0.5 to 1.0 greater than those for foredrag. Since the base is closer to the source of the disturbance, this result should be expected.

Cylindrical model.- For the cylindrical model, the foredrag coefficient was unaffected by the sting support (fig. 9), indicating that the interference field was confined to the cylindrical afterbody. Typical pressure distributions, presented in figure 10, indicate that the interference effects were indeed limited to the rear of the model. The interference effects were quite similar to those of the boattail model, but were smaller. For Mach numbers of 1.2 and higher, the interference effects were negligible, even for $l/D_B = 0$. However, for the model at positions other than symmetrically in line with the free stream, an interference effect would be expected.

The variations of base drag coefficient with l/D_B (fig. 11) were similar to those for the boattail model. However, the increments in base drag coefficient were larger due to the larger base area. Theoretical and experimental values of $(l/D_B)_{cr}$ compare quite well. Variations of $(l/D_B)_{cr}$ for base drag with Mach number (1-inch-diameter sting) are shown in figure 12. The trends are similar to those for the boattail model. The maximum $(l/D_B)_{cr}$ for 1 inch sting and 12° sting flare was 5.5.

Effect of Sting Diameter

Boattail model.- The variations of foredrag coefficient with d/D_B are shown in figure 13. All tests were made at l/D_B ratios greater than critical for all sting diameters in order that the length effects would be negligible. The interference effects were small and, in general, the foredrag decreased with increase in sting diameter. For Mach numbers over 1.10, $(d/D_B)_{cr}$ was approximately 0.65 and at Mach number 1.4, $(d/D_B)_{cr}$ was approximately 1.0 (i.e., no interference). This agrees with the result of reference 3 which showed that there was no foredrag interference due to sting diameter at a Mach number of 1.5. Typical pressure distributions at four d/D_B ratios and the integrated boattail drag values are presented in figures 14 and 15, respectively.

The diameter effect on the base drag coefficient is shown in figure 16. The base drag increased with decreasing d/D_B ratio. At subsonic speeds, there was a small interference effect for all stings tested. At Mach numbers of 1.2 and 1.4, $(d/D_B)_{cr}$ was approximately 0.5. Small discrepancies between the data for the sting and sting plus side support are due to mutual interferences between the two supports.

Cylindrical model.- As would be expected, there was no interference in foredrag due to sting diameter effect for the entire Mach number range (fig. 17). Also, the pressure distributions over the afterbody were not affected by changes in sting diameter as shown in figure 18.

The variations of base drag coefficient with d/D_B are shown in figure 19. It is seen that the base drag was affected by all sting diameters. A mutual interference between the sting and side support is apparent at transonic speeds. Another phenomenon is that the base drag coefficient (i.e., base pressure) changed abruptly when d/D_B changed from zero to a finite value.

CONCLUSIONS

The results of the tests show the following effects of sting-support interference on the foredrag and base drag of the boattail and the cylindrical model:

1. The maximum sting-support interference effects occurred at approximately 0.95 Mach number and were substantially smaller at supersonic speeds.

2. For the boattail model tested, foredrag and base drag data for a sting flare angle of 12° and sting-diameter to base-diameter ratio of 0.87 were free from sting-length interference when the sting length was greater than 6.0 and 6.5 base diameters, respectively. However, there was always an interference on base drag from the sting diameter.

3. For the cylindrical model tested, the foredrag was independent of the sting support. However, the base drag was affected by the sting diameter, but was not affected by sting length for lengths greater than 5.5 base diameters.

Ames Aeronautical Laboratory
National Advisory Committee for Aeronautics
Moffett Field, Calif., Sept. 9, 1957

REFERENCES

1. Tunnell, Phillips J.: An Investigation of Sting-Support Interference on Base Pressure and Forebody Chord Force at Mach Numbers From 0.60 to 1.30. NACA RM A54K16a, 1955.

2. Love, Eugene S.: A Summary of Information on Support Interference at Transonic and Supersonic Speeds. NACA RM L53K12, 1954.

3. Perkins, Edward W.: Experimental Investigation of the Effects of Support Interference on the Drag of Bodies of Revolution at a Mach Number of 1.5. NACA TN 2292, 1951.

4. Chapman, Dean R.: An Analysis of Base Pressure at Supersonic Velocities and Comparison With Experiment. NACA Rep. 1051, 1951. (Supersedes NACA TN 2137)

5. Cahn, Maurice S.: An Experimental Investigation of Sting-Support Effects on Drag and a Comparison With Jet Effects at Transonic Speeds. NACA RM L56F18a, 1956.

6. Hart, Roger G.: Effects of Stabilizing Fins and a Rear-Support Sting on the Base Pressure of a Body of Revolution in Free Flight at Mach Numbers From 0.7 to 1.3. NACA RM L52E06, 1952.

7. Spiegel, Joseph M., and Lawrence, Leslie F.: A Description of the Ames 2- by 2-Foot Transonic Wind Tunnel and Preliminary Evaluation of Wall Interference. NACA RM A55I21, 1956.

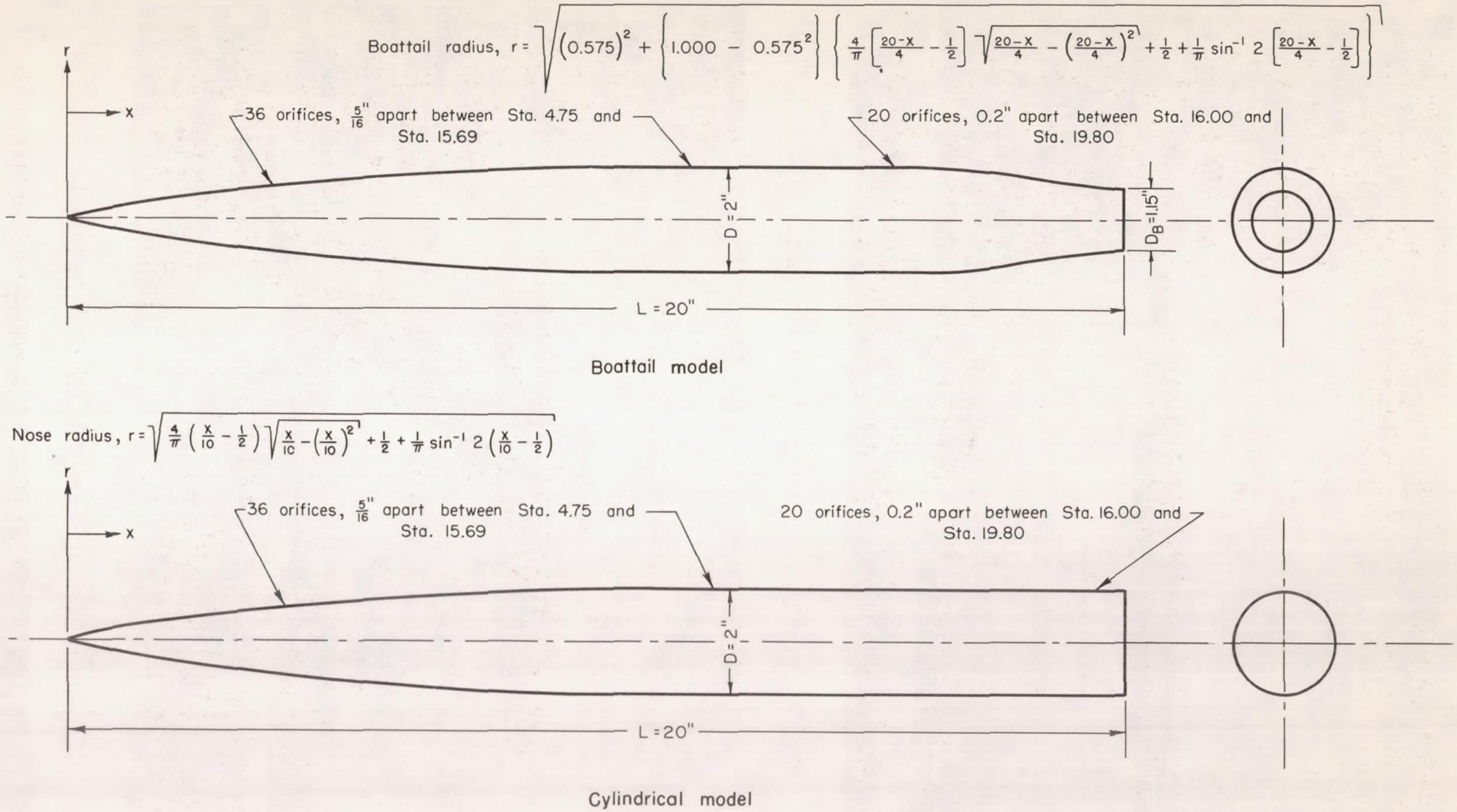

Figure 1.- Geometric details of the boattail and cylindrical models.

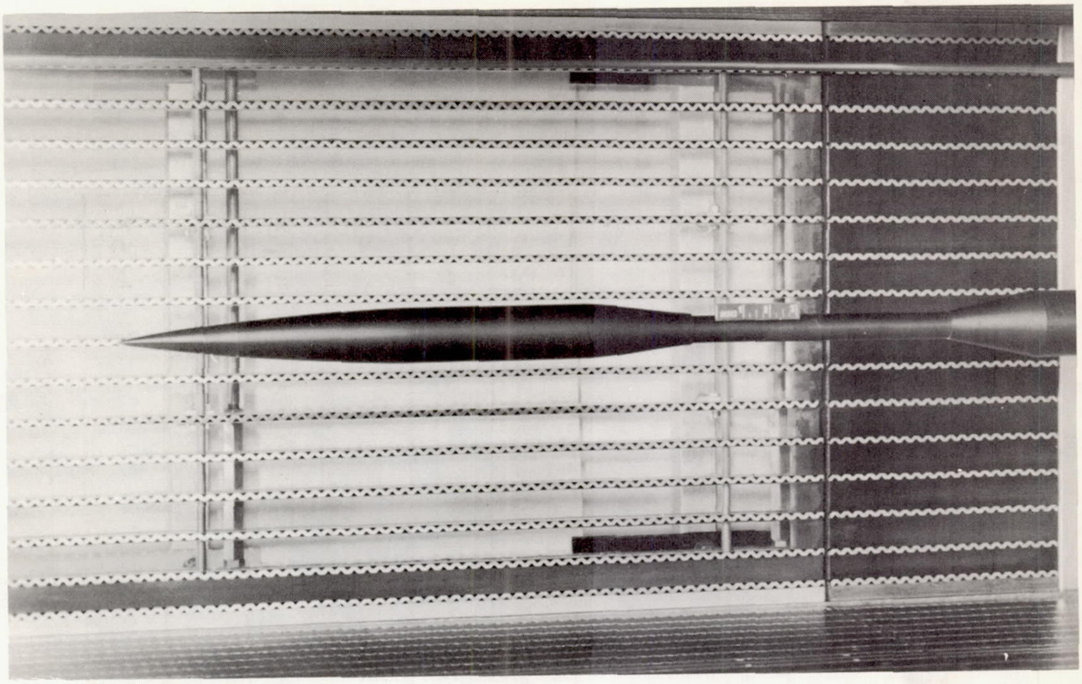

A-21141

(a) Boattail model with sting support.

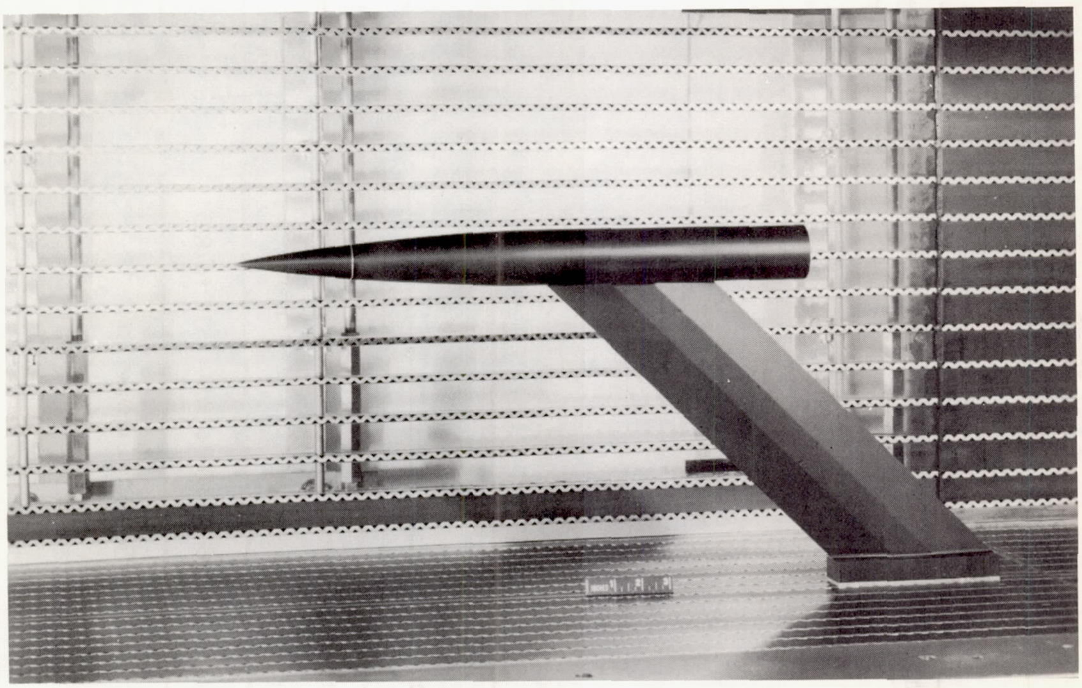

A-21145

(b) Cylindrical model with side support.

Figure 2.- Models and support systems investigated.

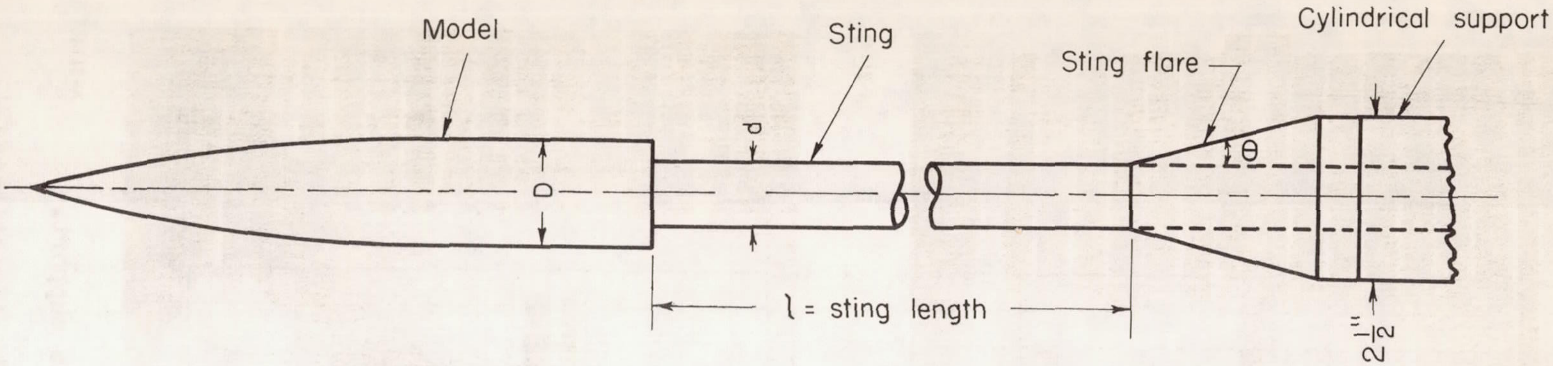

l/D_B range

d \ θ	4°	8°	12°
$\frac{1}{2}$	0.6 to 2.6	0.3 to 5.4	0.7 to 7.4
$\frac{3}{4}$			1.2 to 8.0
1	1.4 to 5.6	1.8 to 6.9	0.1 to 8.5

(a) Boattail model

l/D_B range

d \ θ	4°	8°	12°
$\frac{1}{2}$			0.4 to 3.1
$\frac{3}{4}$			1.1 to 4.5
1	0.8 to 3.3	0.6 to 4.0	0 to 4.9
$1\frac{1}{4}$			1.5 to 5.4
$1\frac{1}{2}$			0.1 to 5.7

(b) Cylindrical model

Figure 3.- Sting support configurations investigated.

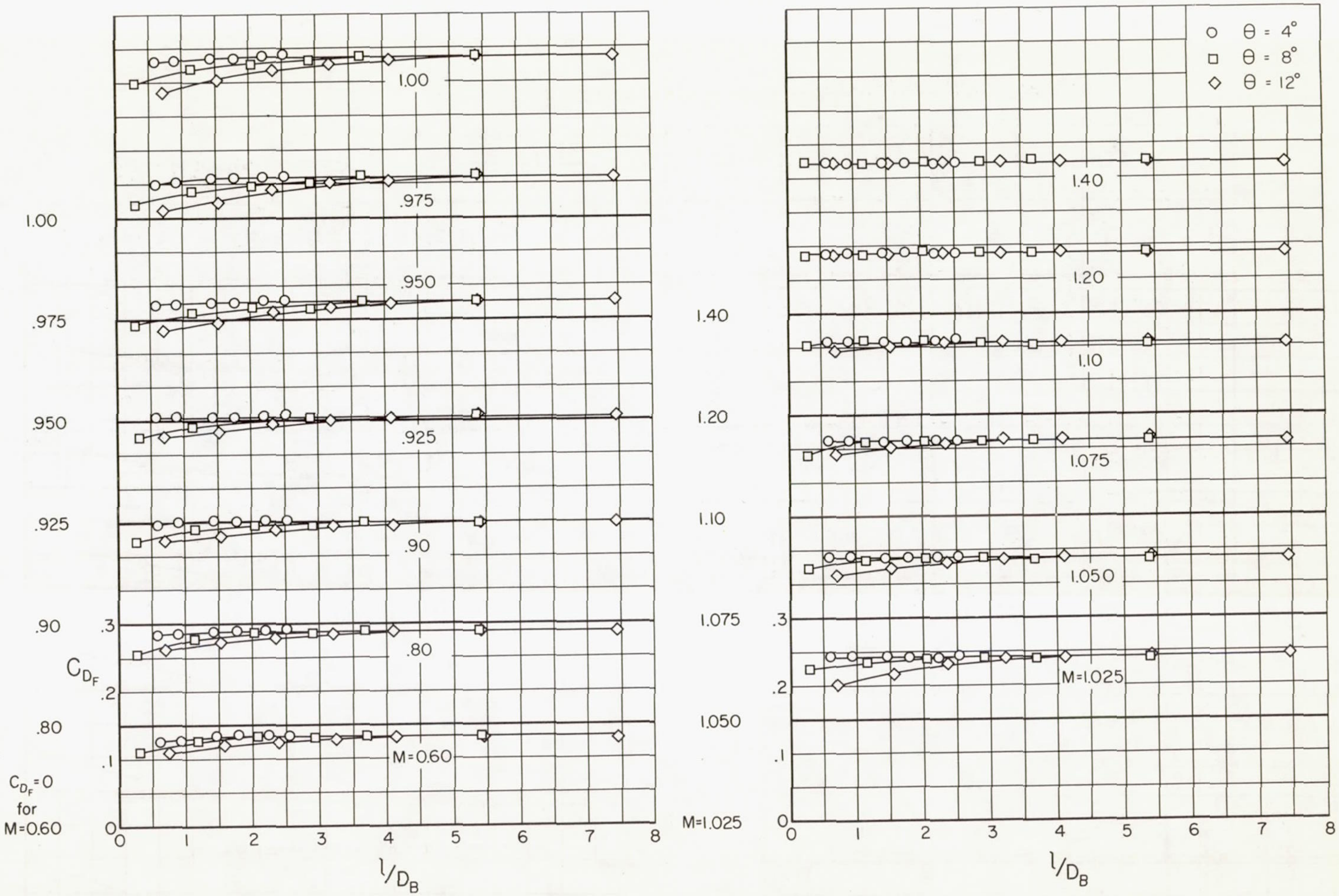

(a) $\frac{d}{D_B} = 0.43$, d = 0.5 in.

Figure 4.- Variations of foredrag coefficient with sting-length to base-diameter ratio; boattail model.

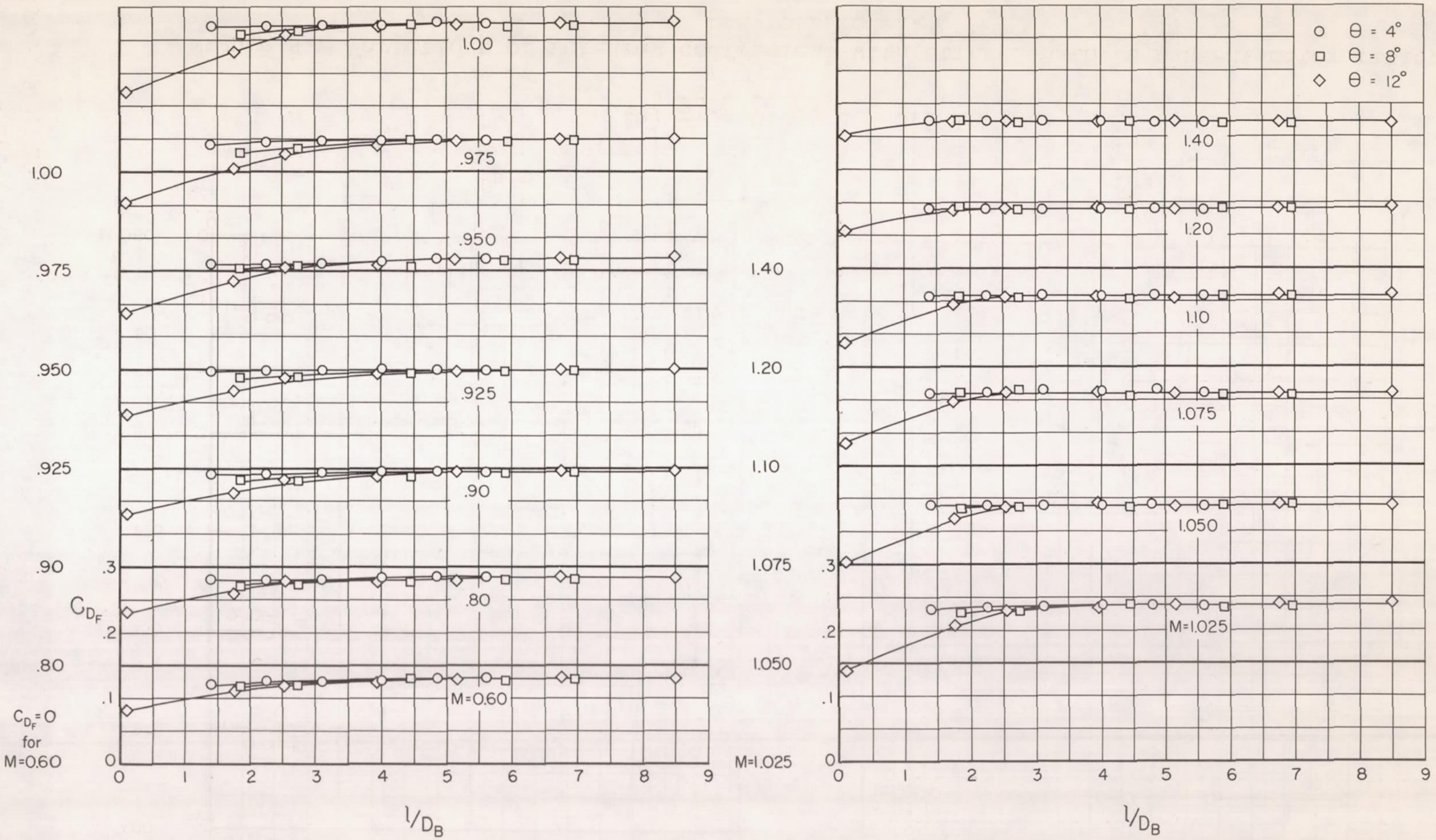

(b) $\frac{d}{D_B}$ = 0.87, d = 1.0 in.

Figure 4.- Concluded.

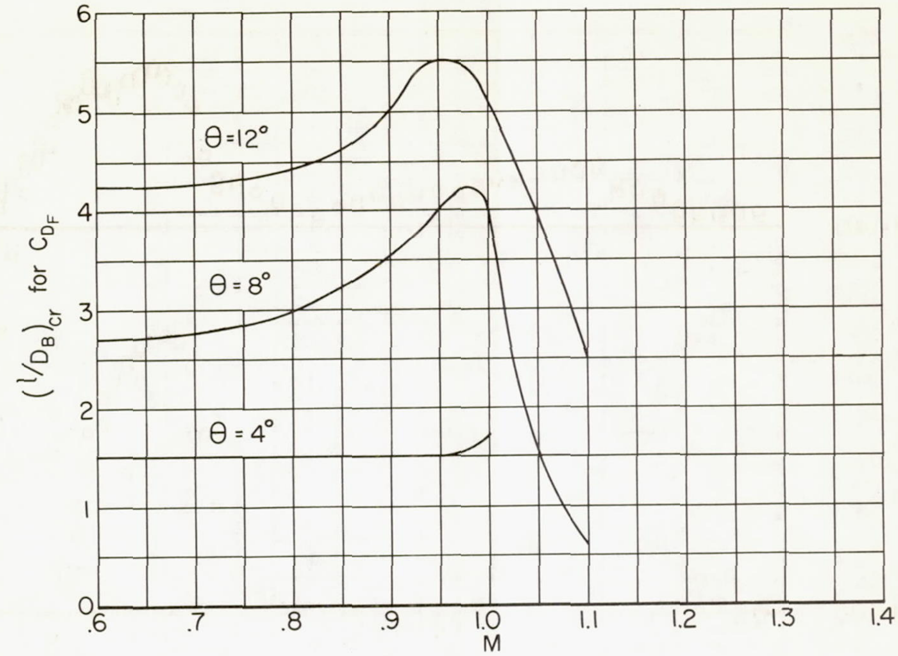

(a) $\frac{d}{D_B}$ = 0.43, d = 0.5 in.

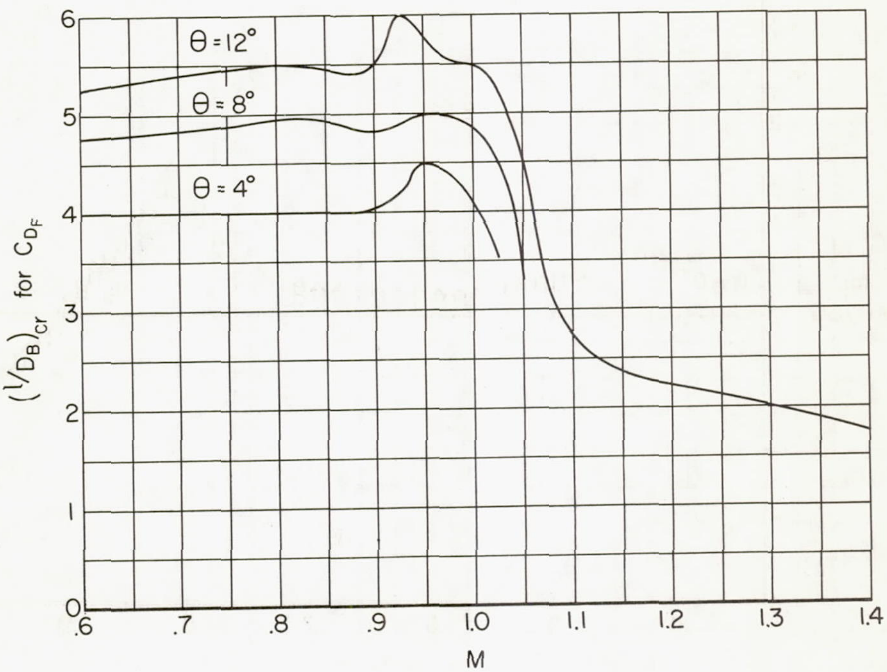

(b) $\frac{d}{D_B}$ = 0.87, d = 1.0 in.

Figure 5.- Variations with Mach number of critical sting-length to base-diameter ratio for foredrag coefficient; boattail model.

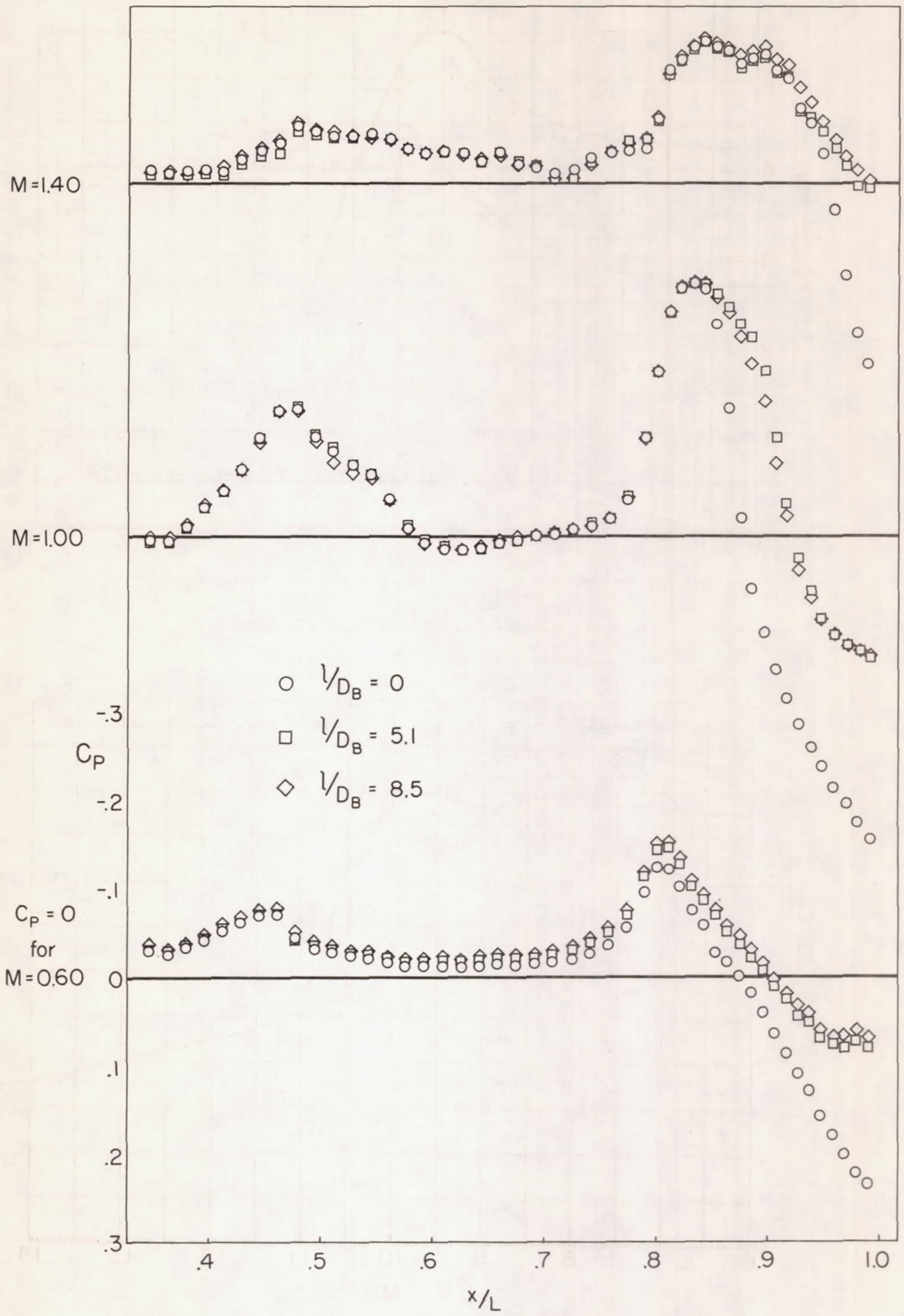

Figure 6.- Typical pressure distributions for three sting-length to base-diameter ratios; boattail model; $d/D_B = 0.87$; d = 1 in.; $\theta = 12^\circ$.

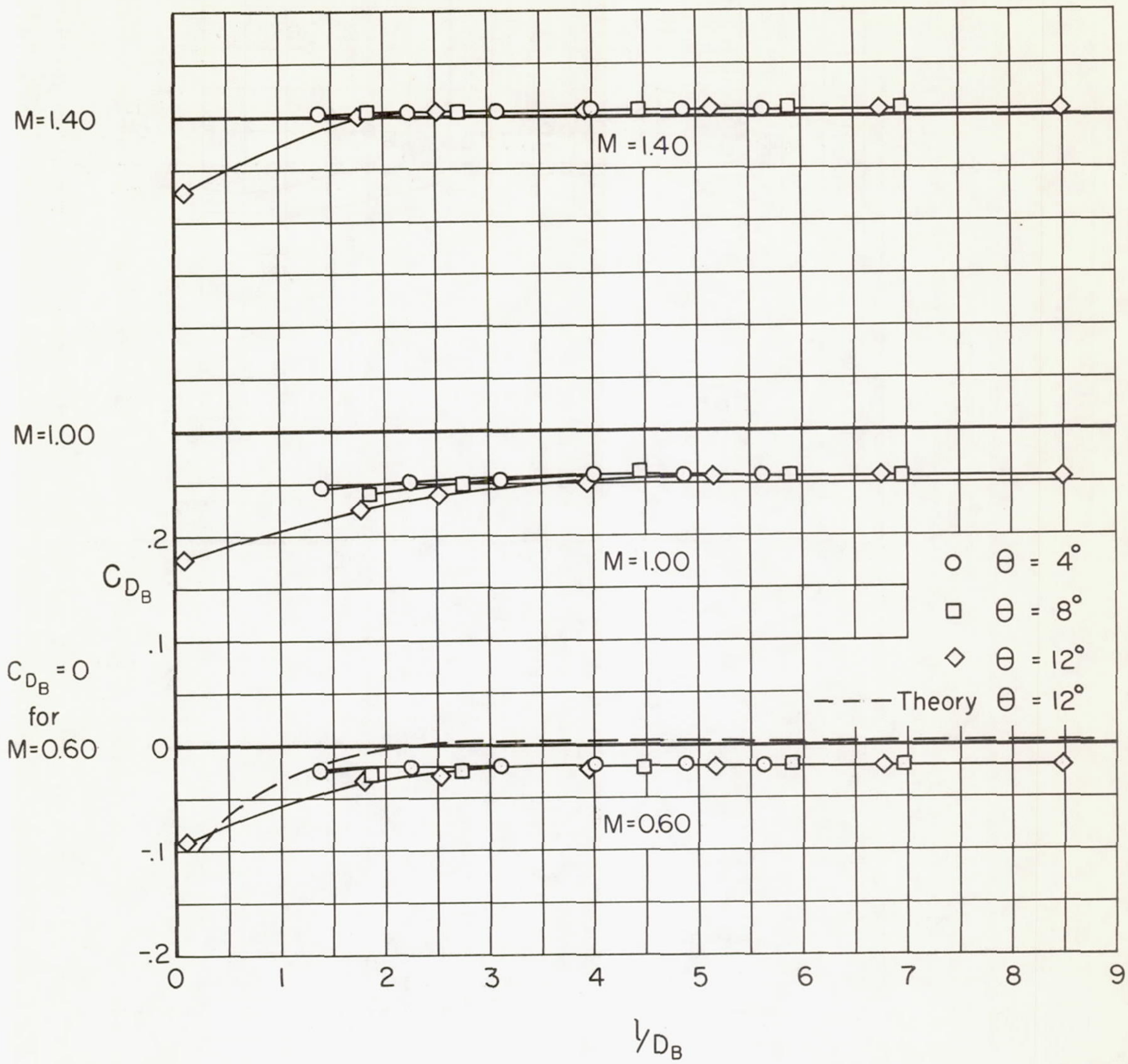

Figure 7.- Typical variations of base drag coefficient with sting-length to base-diameter ratio; boattail model; d/D_B = 0.87; d = 1 in.

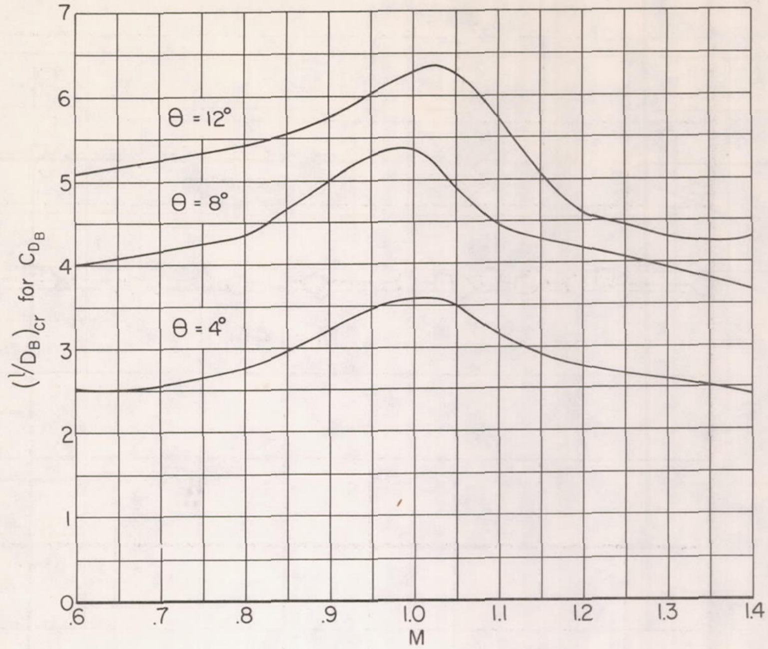

(a) $\frac{d}{D_B} = 0.43$, d = 0.5 in.

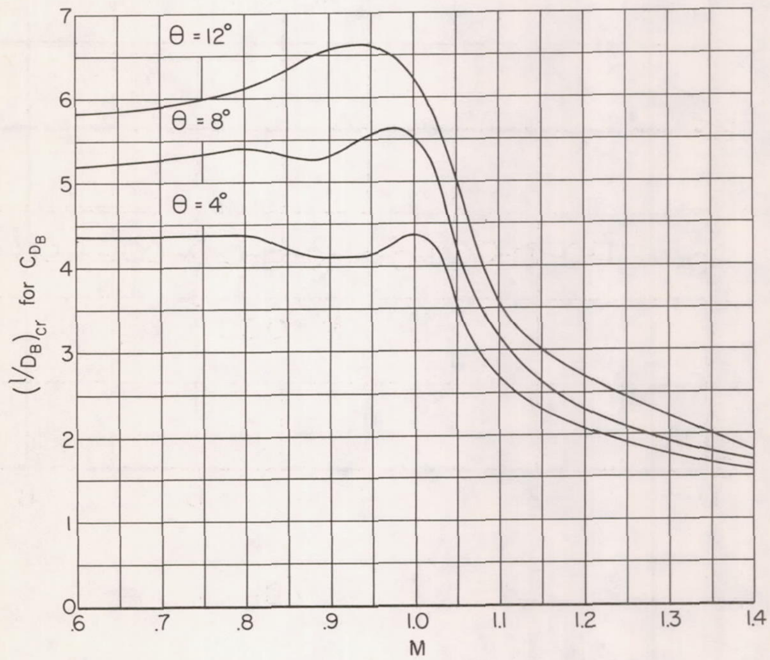

(b) $\frac{d}{D_B} = 0.87$, d = 1.0 in.

Figure 8.- Variations with Mach number of critical sting-length to base-diameter ratio for base drag coefficient; boattail model.

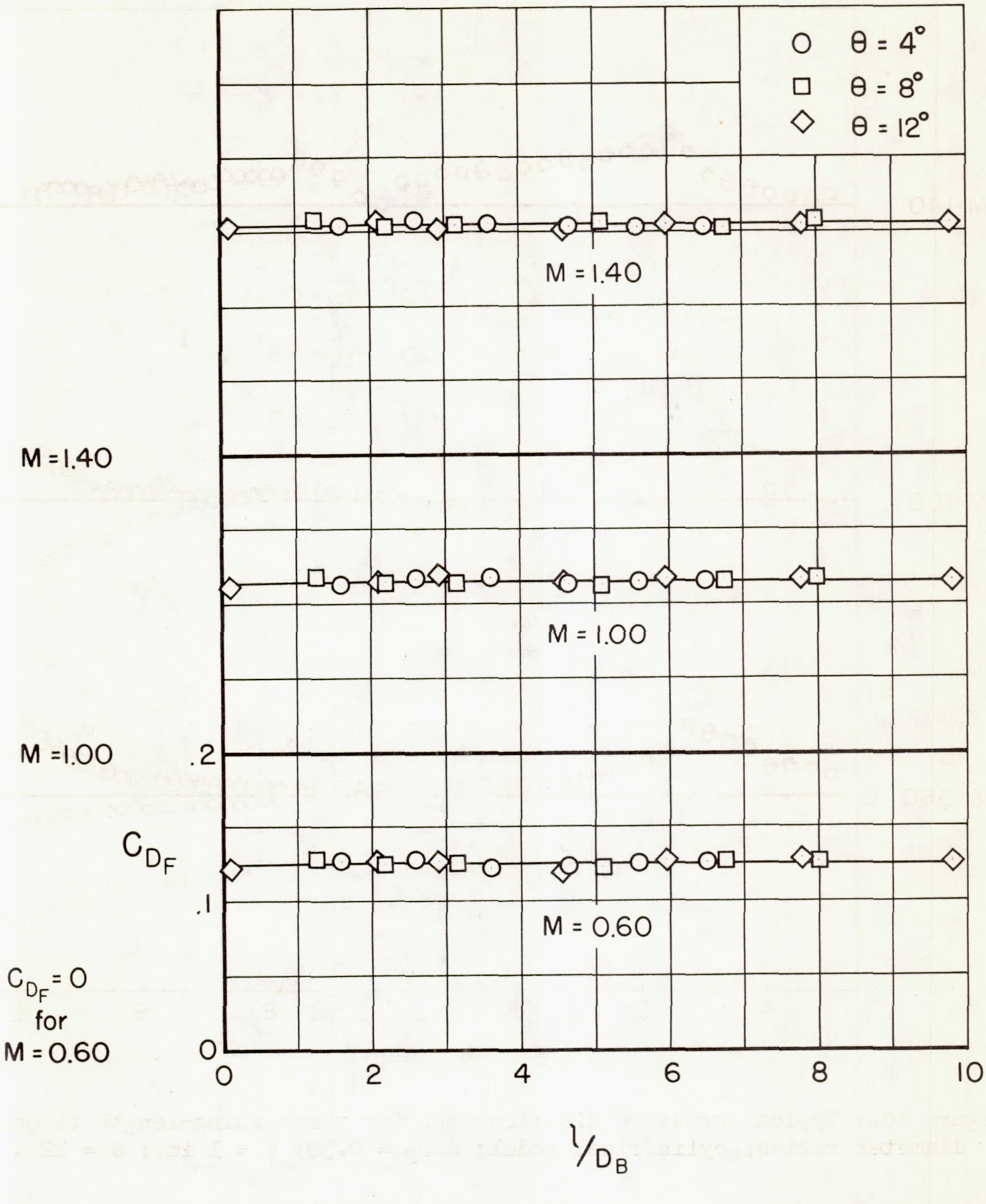

Figure 9.- Typical variations of foredrag coefficient with sting-length to base-diameter ratio; cylindrical model; $d/D_B = 0.50$; d = 1 in.

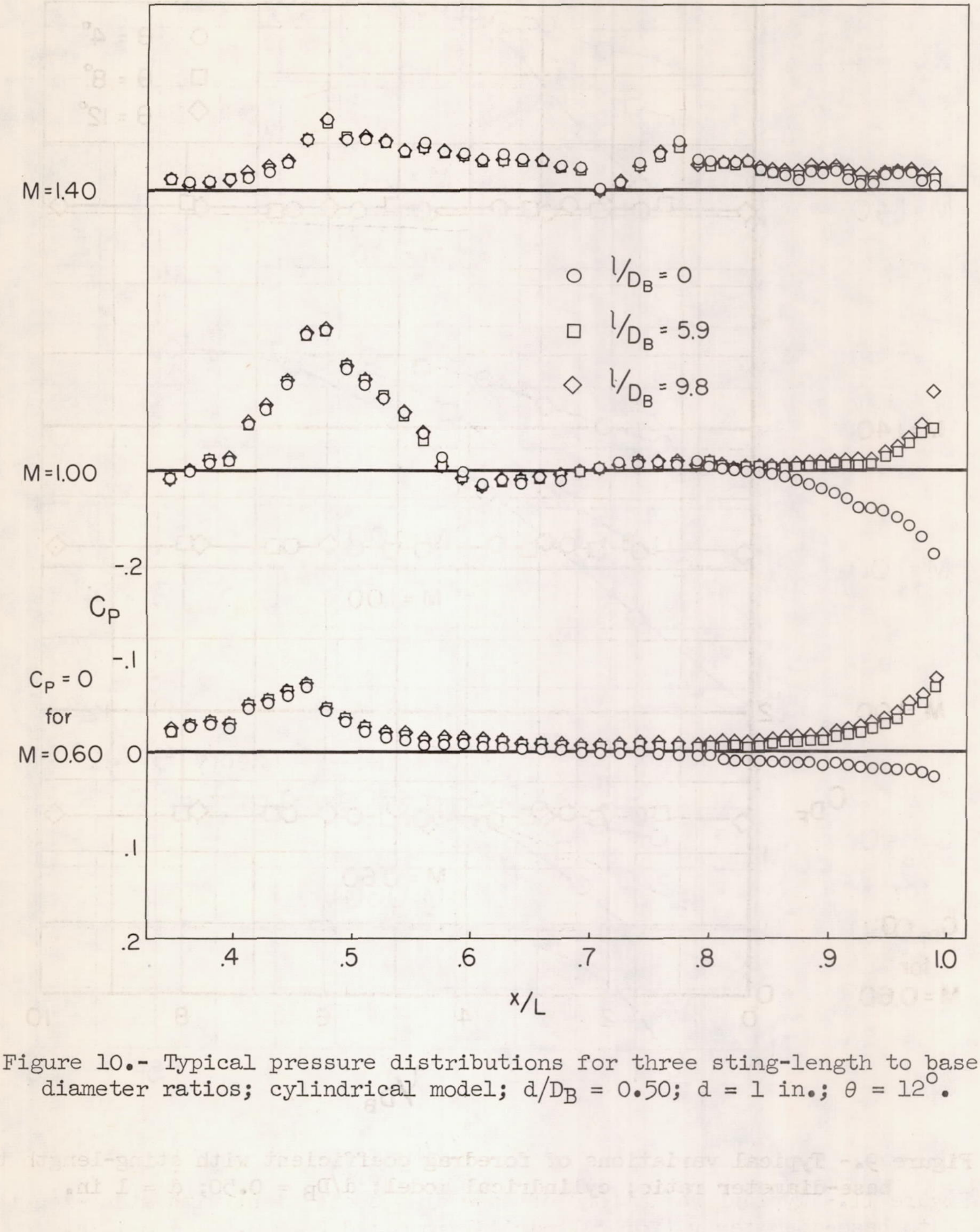

Figure 10.- Typical pressure distributions for three sting-length to base-diameter ratios; cylindrical model; $d/D_B = 0.50$; d = 1 in.; $\theta = 12^{\circ}$.

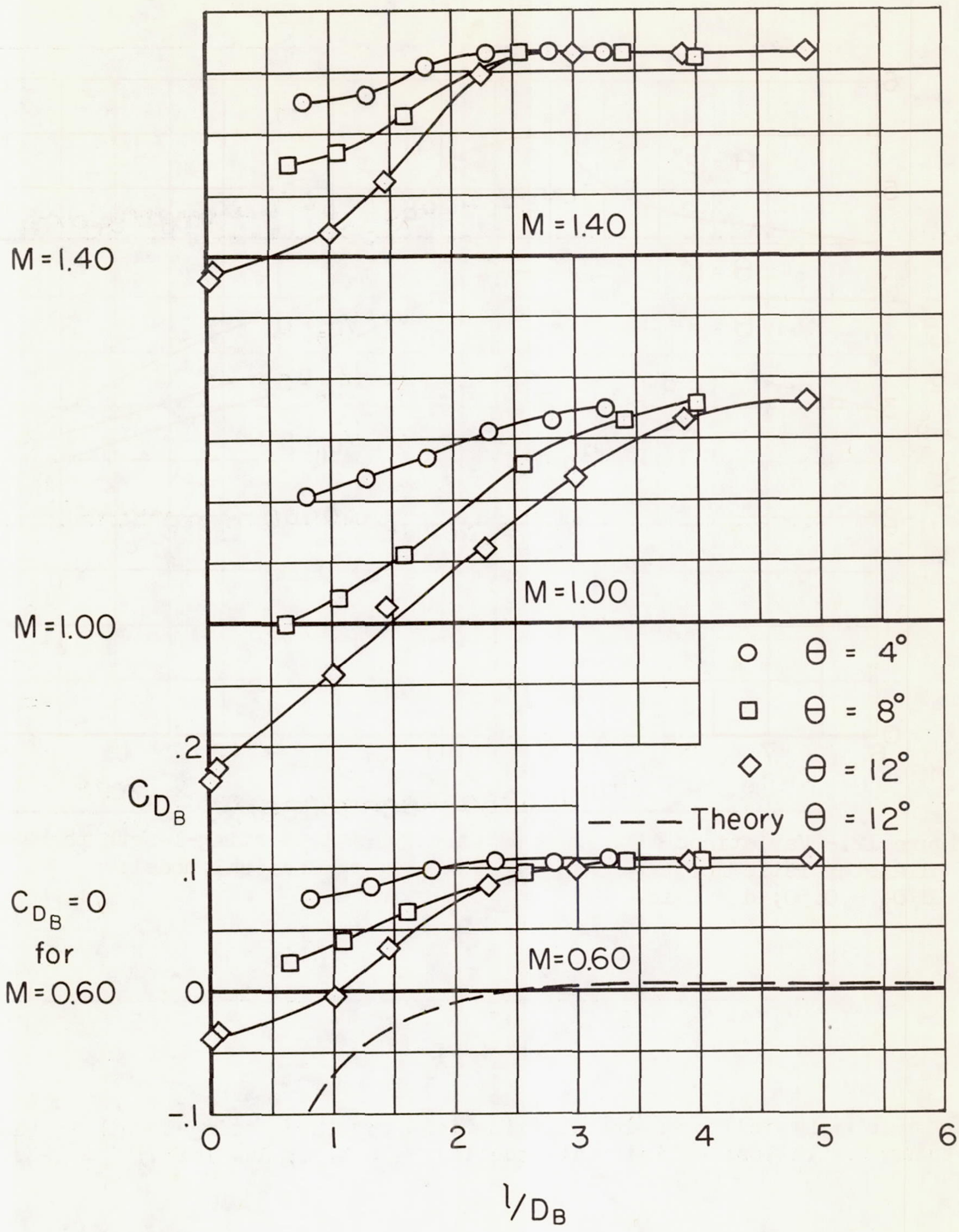

Figure 11.- Typical variations of base drag coefficient with sting-length to base-diameter ratio; cylindrical model; d/D_B = 0.50; d = 1 in.

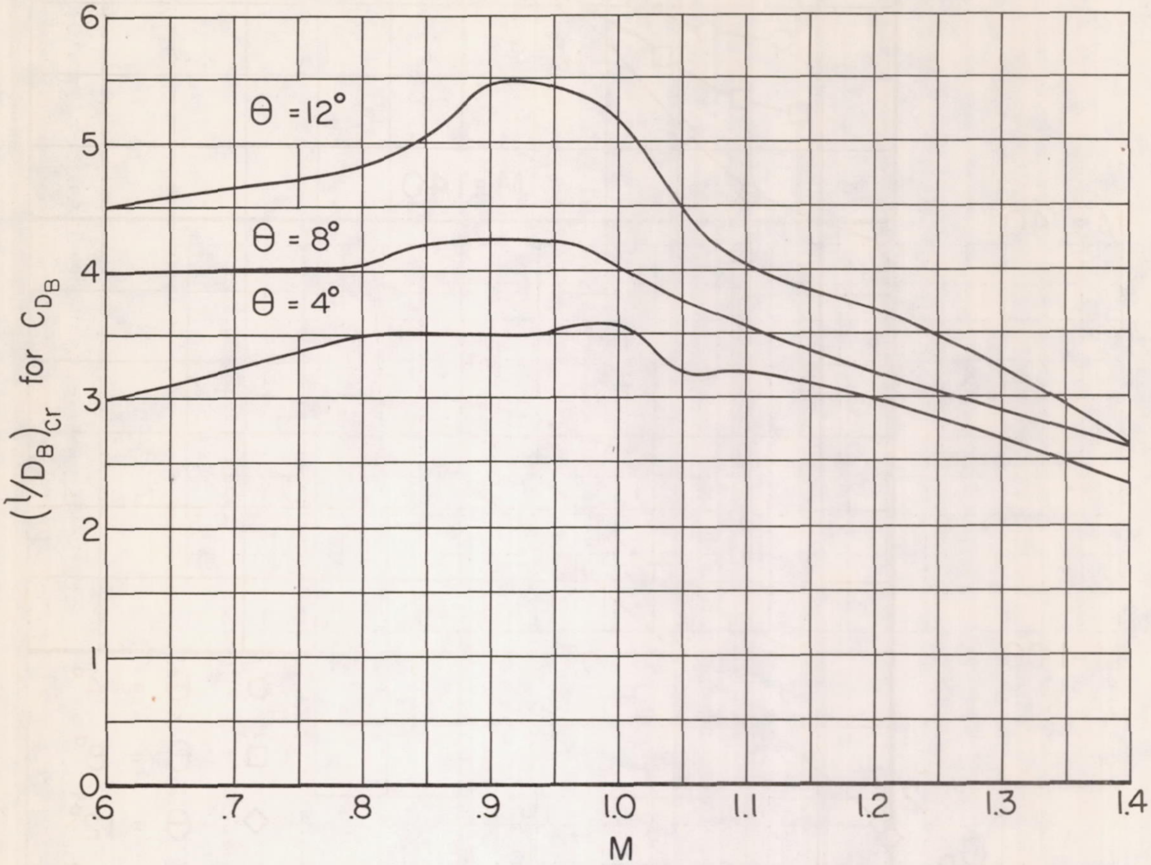

Figure 12.- Variations with Mach number of critical sting-length to base-diameter ratio for base drag coefficient; cylindrical model; $d/D_B = 0.50$; d = 1 in.

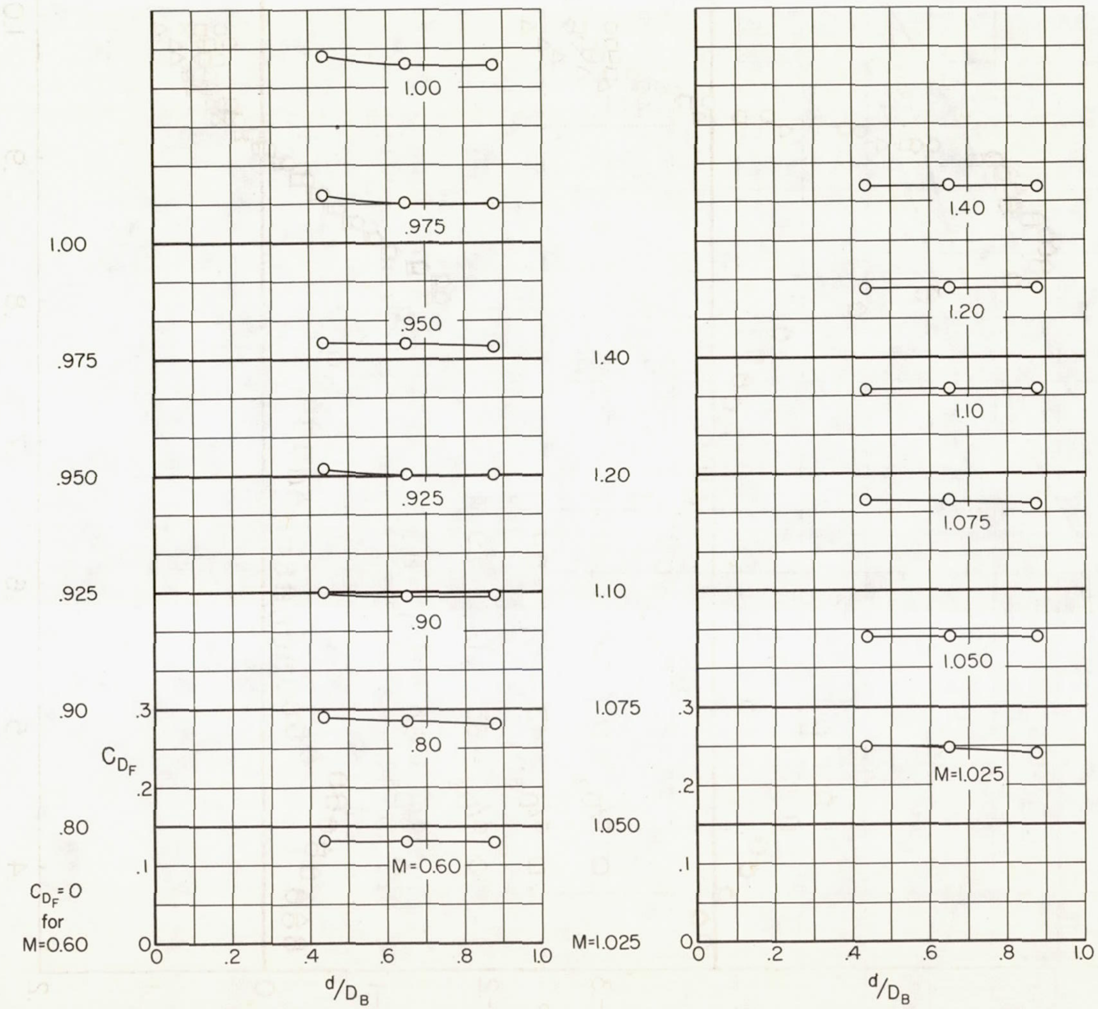

Figure 13.- Variations of foredrag coefficient with sting-diameter to base-diameter ratio; boattail model; $\theta = 12^{\circ}$; $l/D_B > (l/D_B)_{cr}$.

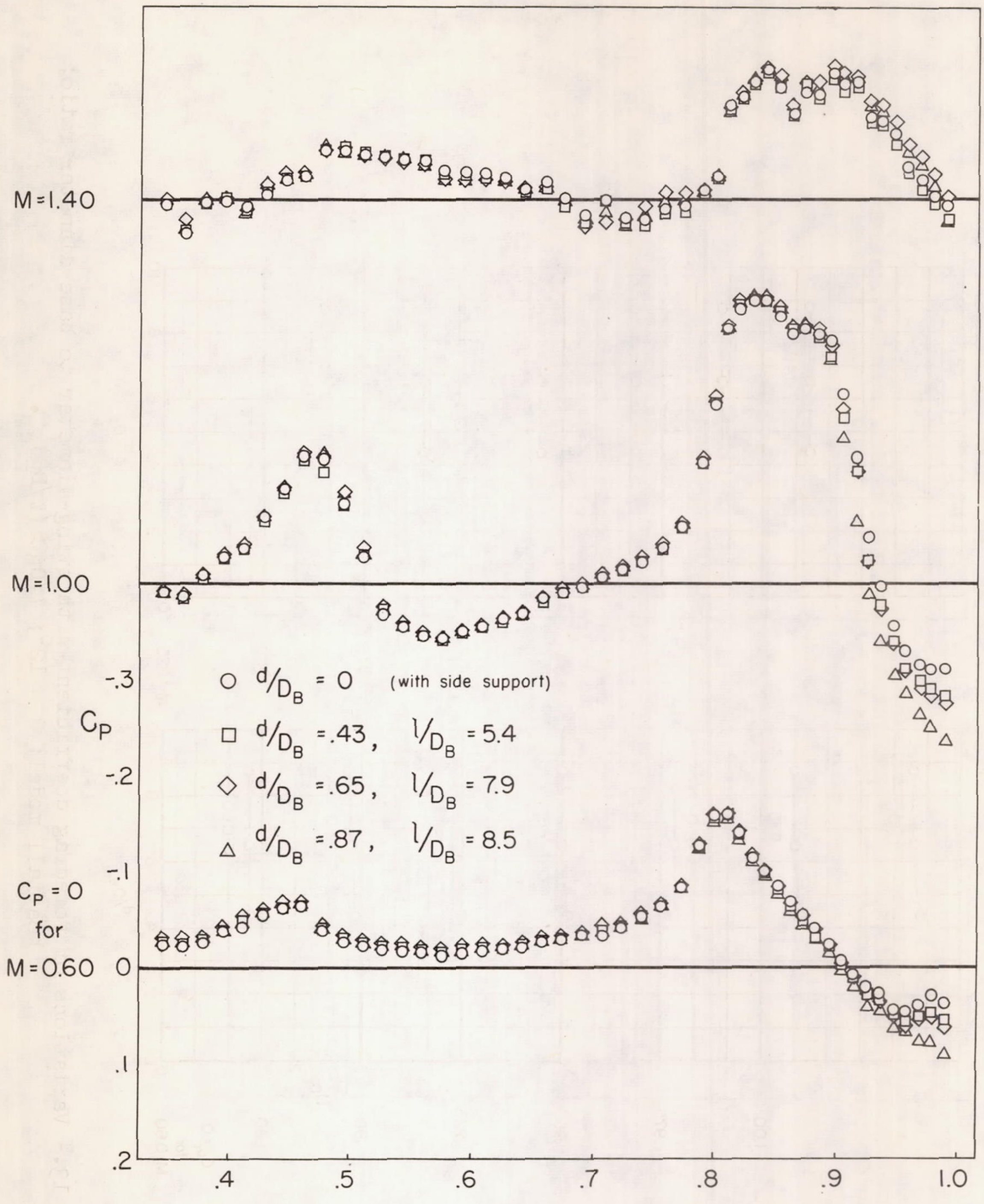

Figure 14.- Typical pressure distributions for four sting-diameter to base-diameter ratios; boattail model; $\theta = 12^{\circ}$; $l/D_B > (l/D_B)_{cr}$.

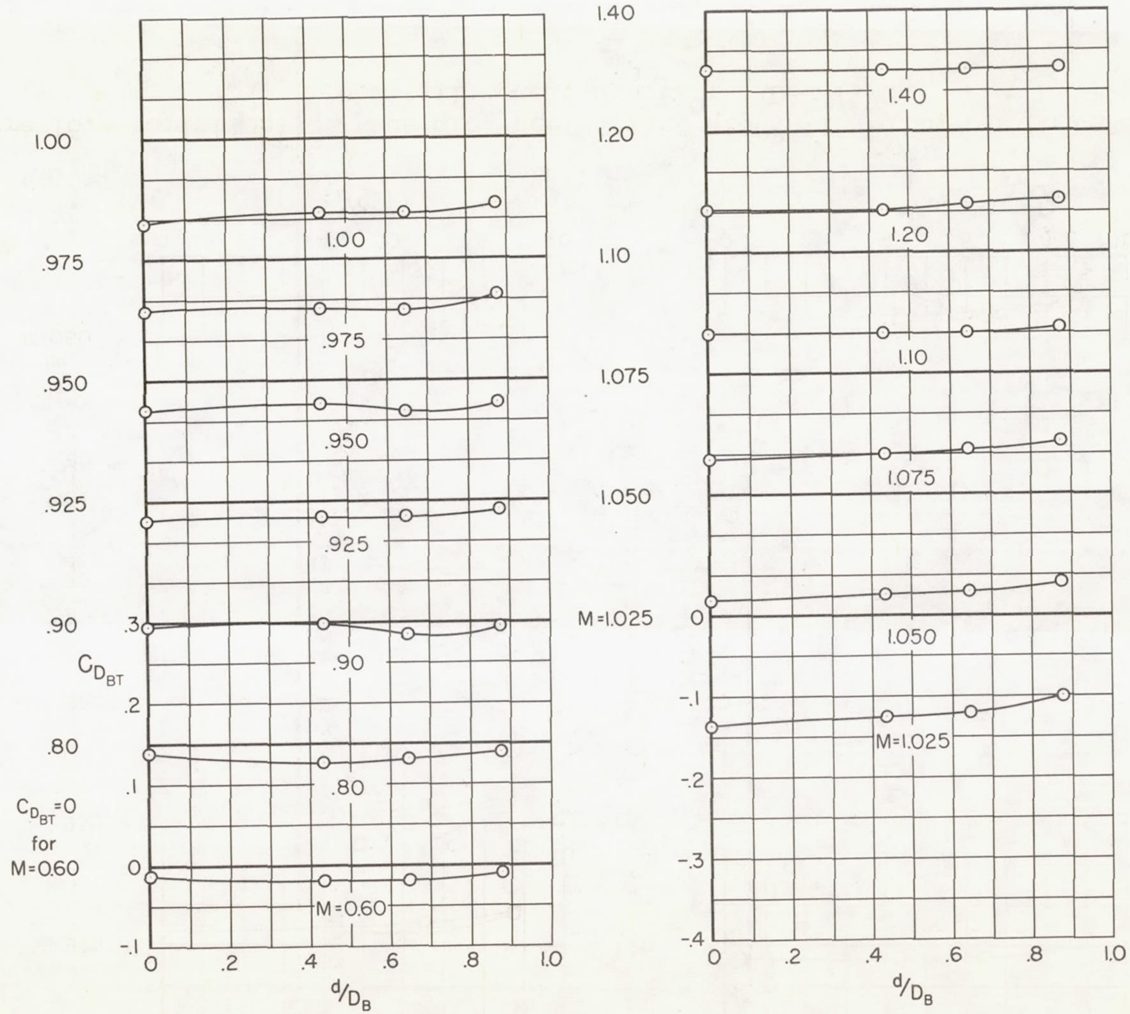

Figure 15.- Variations of boattail drag coefficient with sting-diameter to base-diameter ratio; boattail model; $\theta = 12^{\circ}$; $l/D_B > (l/D_B)_{cr}$.

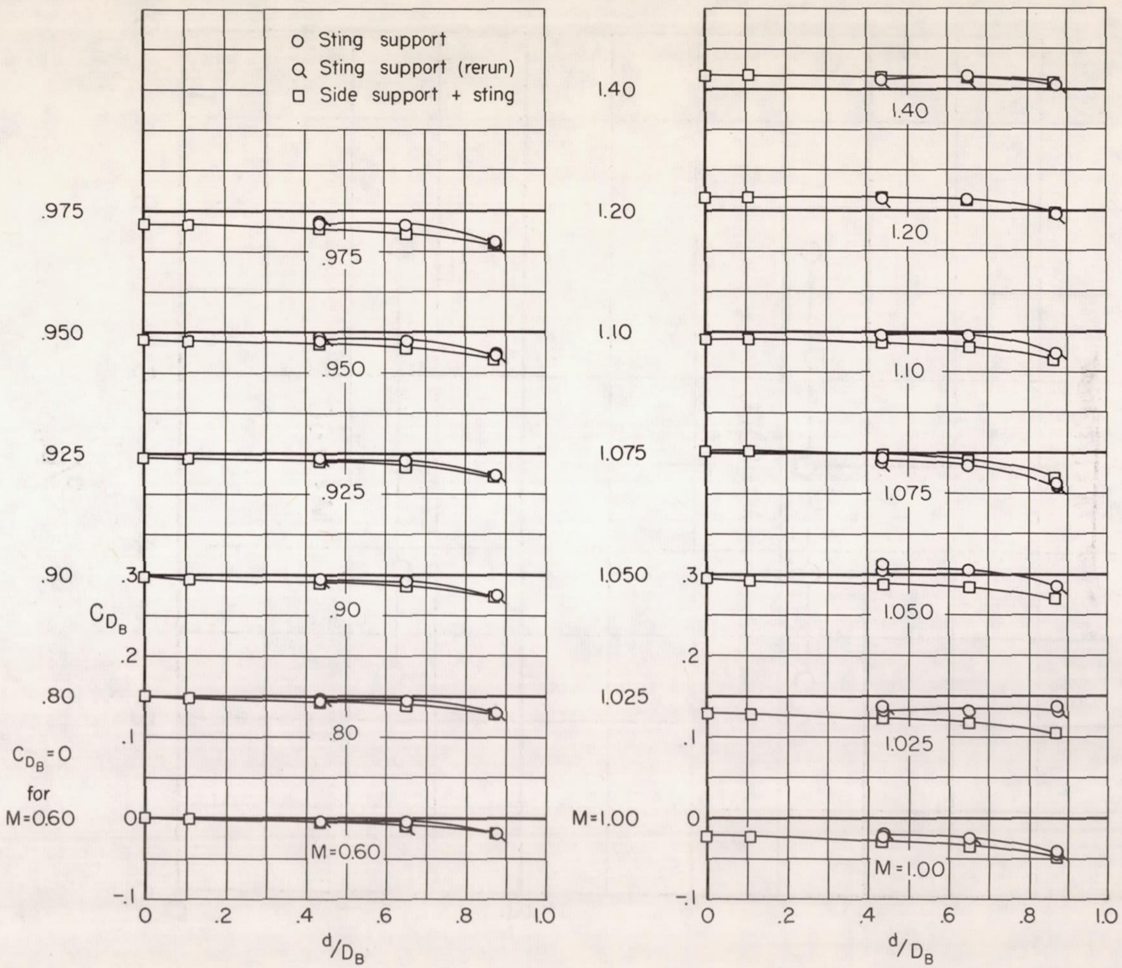

Figure 16.- Variations of base drag coefficient with sting-diameter to base-diameter ratio; boattail model; θ = 12°; $l/D_B > (l/D_B)_{cr}$.

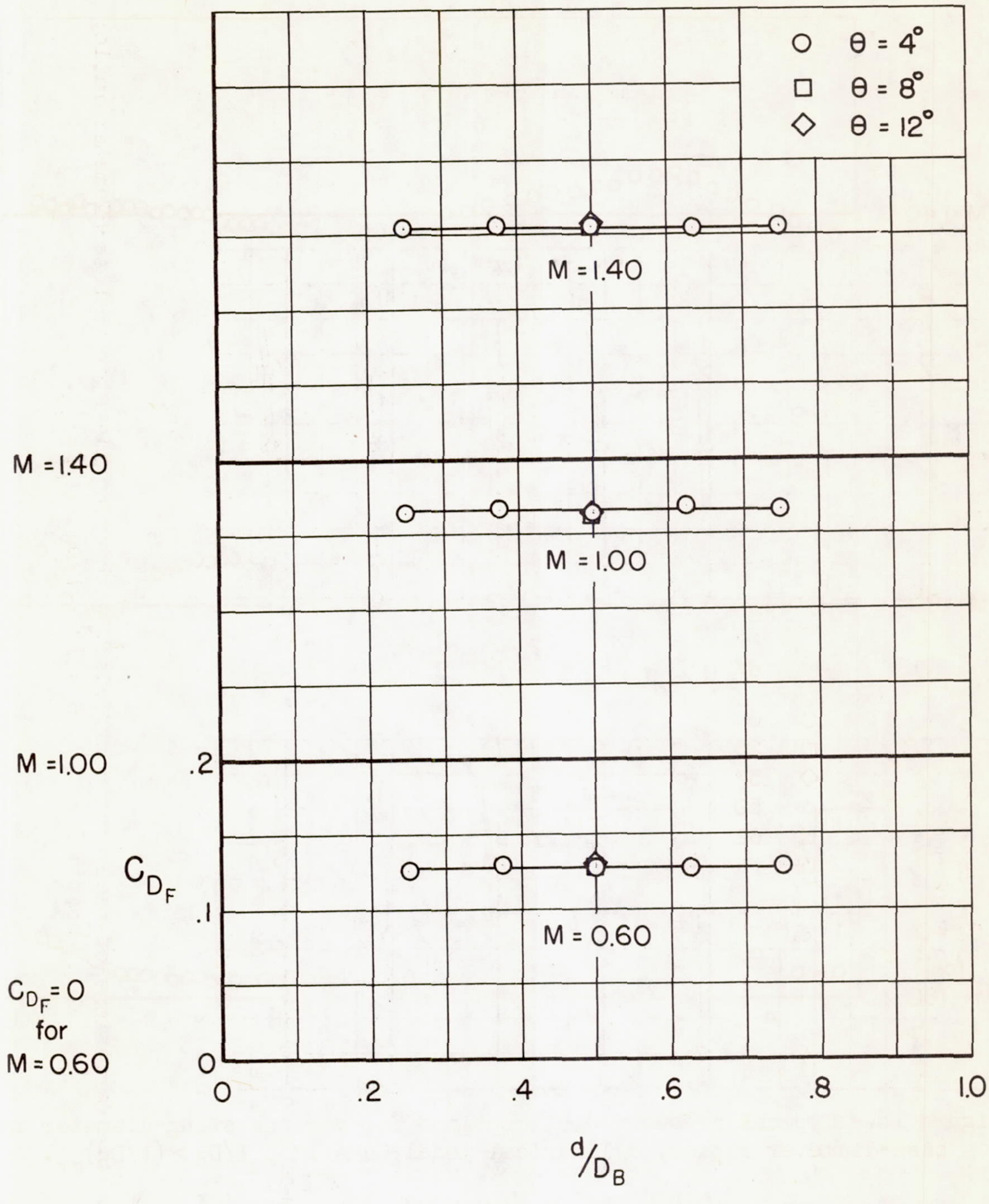

Figure 17.- Typical variations of foredrag coefficient with sting-diameter to base-diameter ratio; cylindrical model; $l/D_B > (l/D_B)_{cr}$.

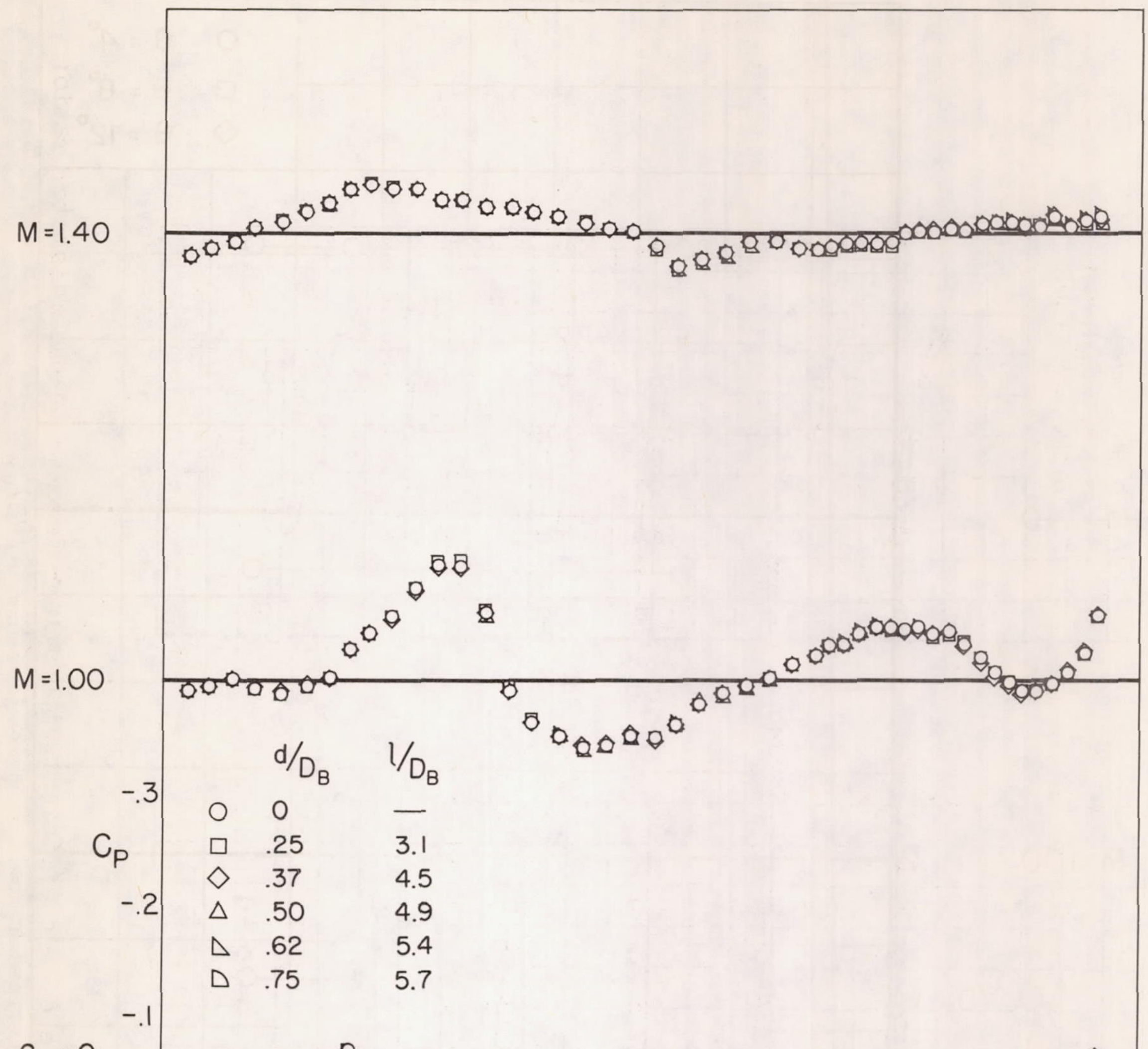

Figure 18.- Typical pressure distributions for various sting-diameter to base-diameter ratios; cylindrical model; $\theta = 12^{\circ}$; $l/D_B > (l/D_B)_{cr}$.

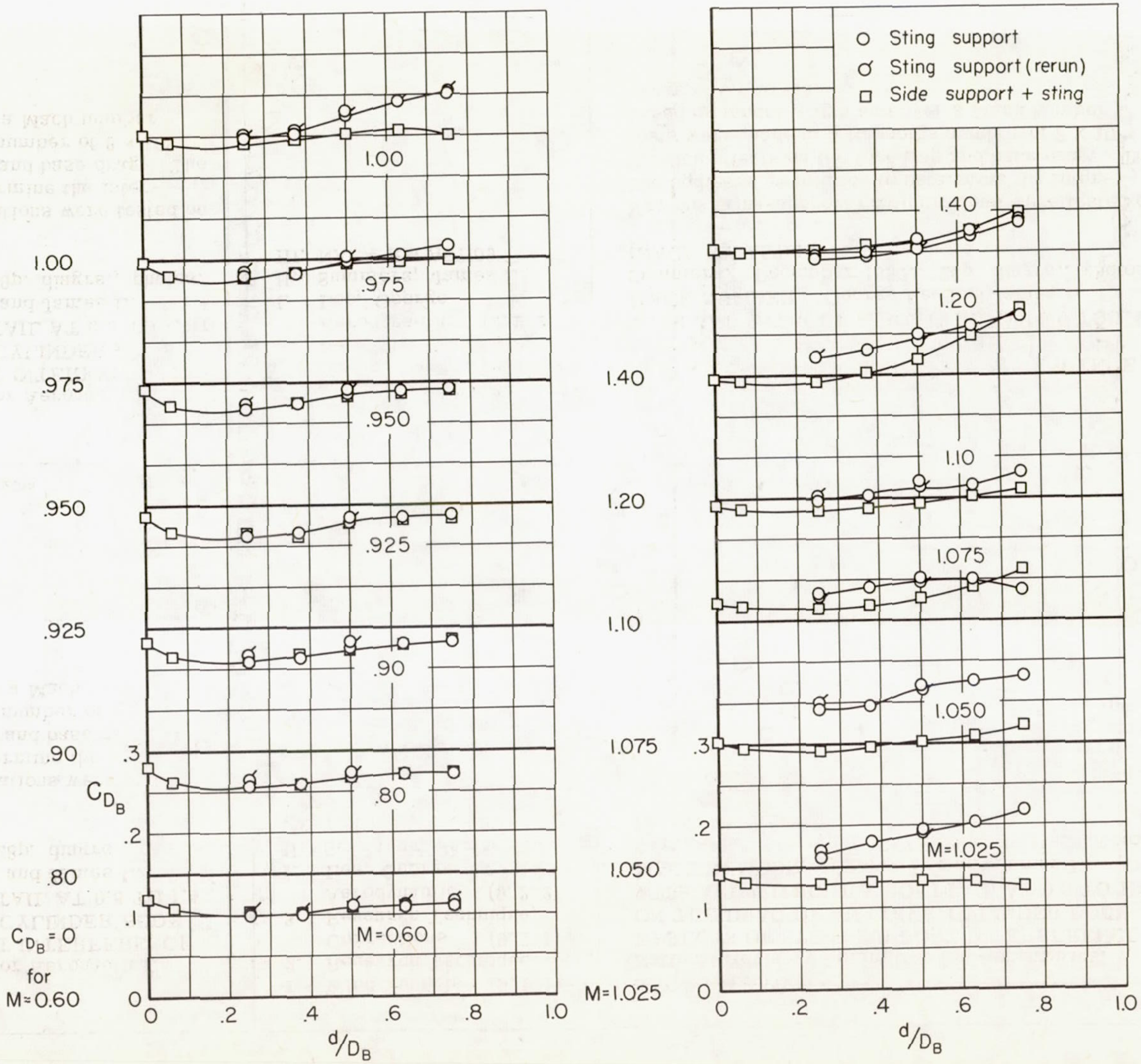

Figure 19.- Variations of base drag coefficient with sting-diameter to base-diameter ratio; cylindrical model; $\theta = 12^{\circ}$; $l/D_B > (l/D_B)_{cr}$.